ELSEVIER

Colloids and Surfaces
A: Physicochemical and Engineering Aspects 93 (1994) 79–95

COLLOIDS AND SURFACES

In situ spectroscopic investigations of adsorbed surfactant and polymer layers in aqueous and non-aqueous systems

P. Somasundaran *, S. Krishnakumar

Langmuir Center for Colloids & Interfaces, Henry Krumb School of Mines, Columbia University, New York, NY 10027, USA

Received 8 December 1993; accepted 15 March 1994

Abstract

Adsorption of surfactants and polymers at the solid–liquid interface is used widely to modify interfacial properties in a variety of industrial processes such as flotation, ceramic processing, flocculation/dispersion, detergency and enhanced oil recovery. A molecular level understanding of the structure of the adsorbed layer is beneficial for improving these processes by manipulating the adsorbed layer. In this paper we discuss the use of fluorescence, electron spin resonance (ESR) and Raman spectroscopy for the study of adsorbed surfactant and polymer layers in aqueous and non-aqueous systems. For example, fluorescence studies using pyrene probe on adsorbed surfactant and polymer layers in aqueous systems along with ESR and Raman spectroscopy reveal the role of surface aggregation and conformation of the adsorbed molecules in controlling the dispersion and wettability properties of the system. In non-aqueous systems, ESR studies using paramagnetic nitroxide probes show how the adsorption of water affects the conformation of adsorbed surfactant molecules and thus affects their dispersion properties.

Keywords: Electron spin resonance; Fluorescence; Non-aqueous dispersions; Polymer conformation; spectroscopy

Introduction

Interfaces are commonly encountered in nature and have become an integral part of all human endeavors both scientific and technological. Of all the interfaces known the solid–liquid interface is the most important owing to its involvement in several biological and industrial processes. Adsorption of surfactants and polymers at the solid–liquid interface is discussed usually in connection with processes like flotation and flocculation as the surface modification caused by the adsorption is mainly responsible for the efficiency of these processes [1,2].

Understanding the micro- and nano-structure of the adsorbed layer at the solid–liquid interface is helpful for utilizing adsorption to enhance many processes dependent on adsorption by designing the adsorbed layers for optimum configurational characteristics. Until recently methods of surface characterization were limited to measurement of macroscopic properties like adsorption density, zeta potential, wettability etc. Such studies, while being helpful to provide an insight into the mechanisms, could not yield any direct information on the microscopic characteristics of the adsorbed species. Recently spectroscopic techniques have been developed for characterizing the adsorbed layers of surfactants and polymers at the solid–liquid interface and for the identification of surface

*Corresponding author.

SSDI 0927-7757(94)02897-2

compounds on mineral particles. In this paper the applications of fluorescence, electron spin resonance (ESR) and Raman spectroscopic techniques to probe the microstructure of the adsorbed layers of surfactants and polymers on minerals in aqueous and non-aqueous media are discussed. This paper encompasses a review of some of the past work and some of our recent attempts to delineate the role of microstructures of adsorbed surfactants and polymers on solid surfaces.

2. Fluorescence spectroscopy

Fluorescence emission is the radiative emission of light by an excited molecule returning to its ground state energy level. This phenomenon bears a wealth of information on the environment of the light absorbing species and has been exploited for a long time for exploring the solution behavior of surfactants. Parameters of fundamental importance in fluorescence emission are (1) emission maximum (wavelength of maximum intensity), (2) quantum yield of fluorescence (emission efficiency measured as intensity) and (3) fluorescence lifetime (time taken by the excited state to decay to $1/e$ of its initial value).

The fluorescence measurements are generally carried out by a steady state fluorescence spectrofluorometer and lifetime of fluorescence by a time-resolved fluorescence lifetime instrument [3]. The dependence of fluorescence intensity and lifetime on the physicochemical environment of the fluorescing molecule has been well documented [4]. Such data have been applied to micellar photochemistry to understand the property of micelles [5]. We have recently adapted this technique as a tool for the adsorbed layer of surfactants on solids to obtain information on the *micropolarity, microviscosity of the probe environment and the aggregation number of the surfactant at the interface.* To determine the micropolarity a fluorescent molecule, like pyrene, which possesses a highly structured fluorescence spectrum whose vibrational lines are susceptible to intensity fluctuations brought on by polarity changes of the medium, is used. This empirical knowledge has been found to be of universal applicability and used widely to investigate the micropolarity of micelles. A properly resolved fluorescence spectrum of pyrene in fluids has five vibrational fine structures in the region from 370 to 400 nm (Fig. 1). The intensities of the first (I_1) and the third (I_3) are found to be

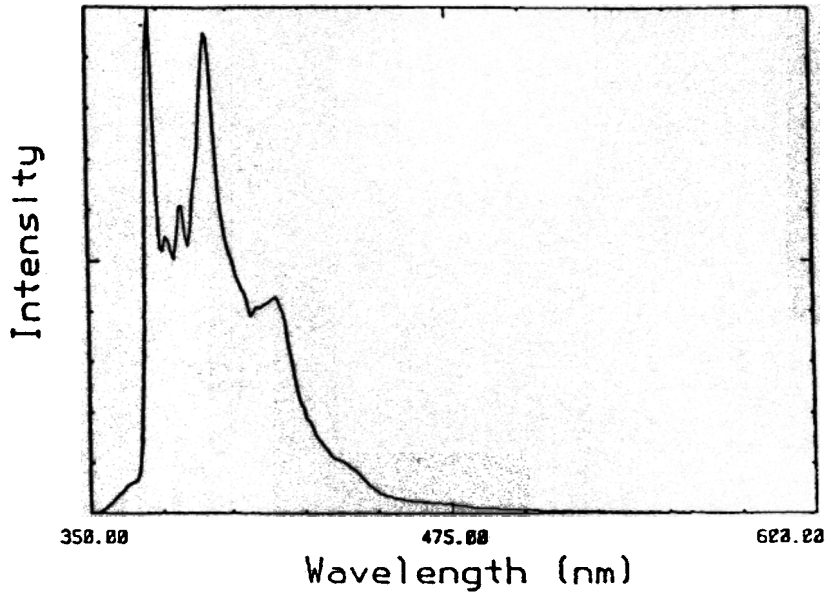

Fig. 1. Typical fluorescence spectrum of pyrene showing the five vibrational lines.

particularly sensitive to the changes in the probe environment. The ratio of these peaks (I_3/I_1), sometimes referred to as the polarity parameter, changes from about 0.6 in water to a value greater than unity in hydrocarbon media.

2.1. Adsorption of sodium dodecyl sulfate on alumina

The adsorption of sodium dodecyl sulfate (SDS) on alumina from aqueous solutions has been extensively studied and used as a model system here to exemplify the different stages in the mechanisms of adsorption of an ionic surfactant on a charged mineral. A careful analysis of such an isotherm was first done by Somasundaran and Fuerstenau and is referred to as the S–F isotherm. A typical example of an S–F isotherm is shown in Fig. 2, where the adsorption of SDS on alumina at pH 6.5 under a constant salt concentration of 10^{-1} kmol m^{-3} is shown [6]. Mechanistically, these regions may be viewed as follows.

Region I which has a slope of unity under constant ionic strength conditions is characterized by the existence of electrostatic interactions between the ionic surfactant species and the oppositely charged solid surface.

Region II is marked by a conspicuous increase in adsorption which is attributed to the onset of surfactant aggregation at the surface through lateral interactions between hydrocarbon chains. This phenomenon is referred to as hemi-micelle formation [7,8]. The colloidal aggregates formed on the surface in general between surfactant and/or polymer species are referred to as *solloids* (surface colloids) [9]. In the case of simple ionic surfactants they have also been called hemi-micelles, admicelles, surface micelles and surfactant self-assemblies [10].

Region III shows a decrease in the slope of the isotherm and this is ascribed to the increasing electrostatic hindrance to the surfactant adsorption following interfacial charge reversal caused by the adsorption of the charged species. In Region III and beyond, both the adsorbent species and the adsorbate are similarly charged.

Region IV and the plateau in it correspond to the maximum surface coverage as determined by

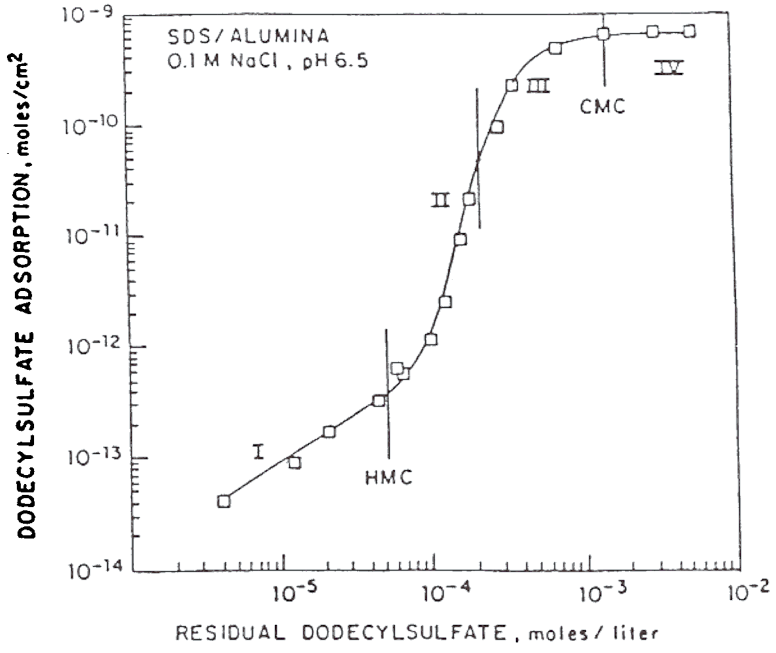

Fig. 2. Adsorption isotherm of sodium dodecyl sulfate (SDS) on alumina at pH 6.5 in 10^{-1} kmol m^{-3} NaCl.

micelle formation in the bulk or monolayer coverage whichever is attained at the lowest surfactant concentration; further increase in surfactant concentration does not alter the adsorption density. A schematic representation of adsorption by lateral interactions is given in Fig. 3.

Classical methods based on zeta potential, adsorption density and hydrophobicity, referred to as bulk methods, help to generate an overall picture of the adsorption process. The application of spectroscopic techniques to study these systems gives a better insight into the interior of the Al_2O_3/SDS solloid system. The I_3/I_1 values for pyrene were determined for alumina/sodium dodecyl sulfate/water systems for various regions of the adsorption isotherm. The data shown in Fig. 4 are

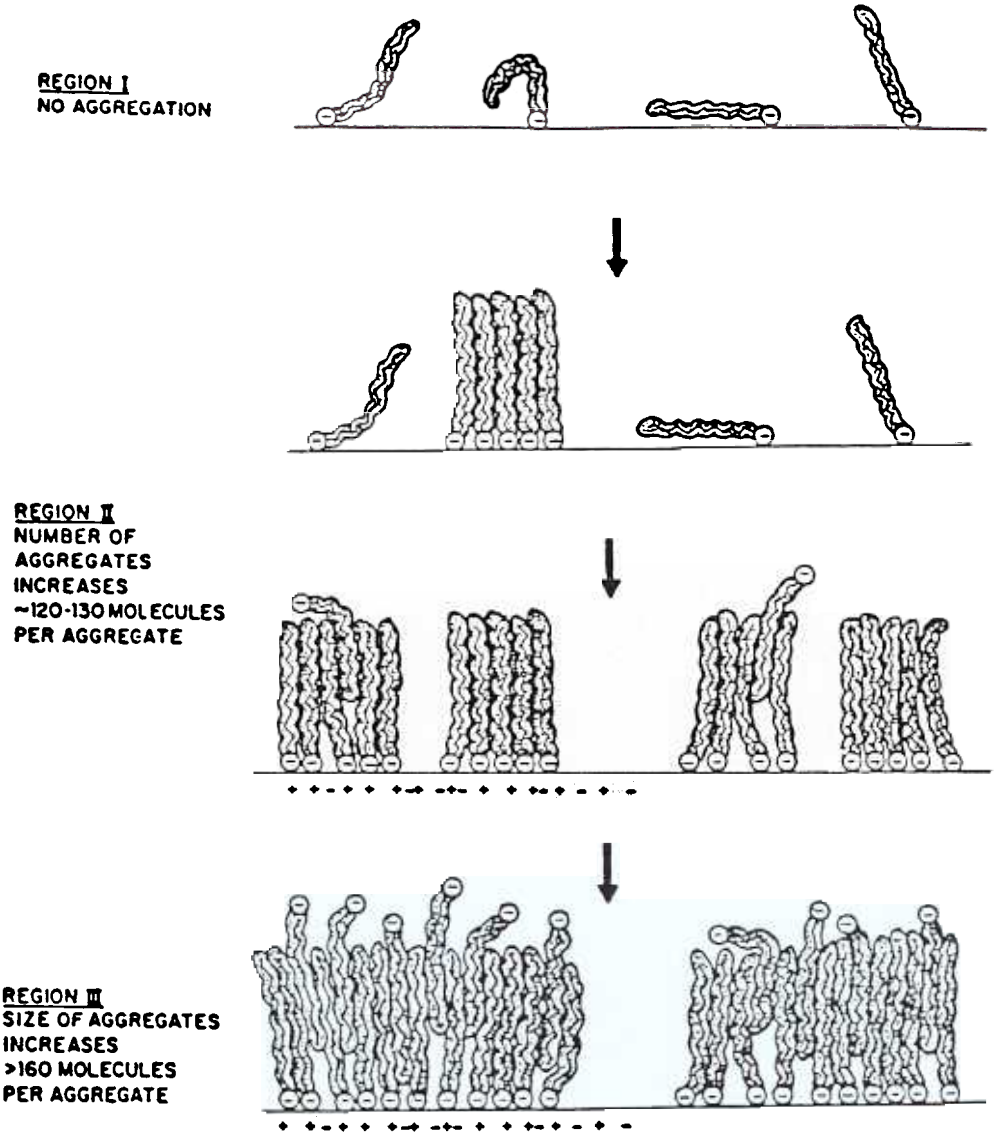

Fig. 3. Schematic representation of the correlation of surface charge and the growth of aggregates for various regions of th adsorption isotherm depicted in Fig. 2.

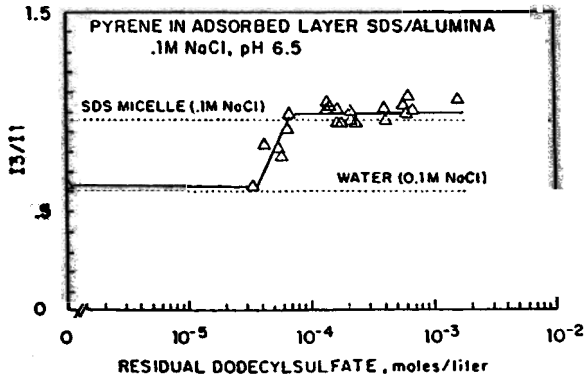

Fig. 4. I_3/I_1 fluorescence parameter of pyrene in sodium dodecyl sulfate (SDS) in alumina slurries.

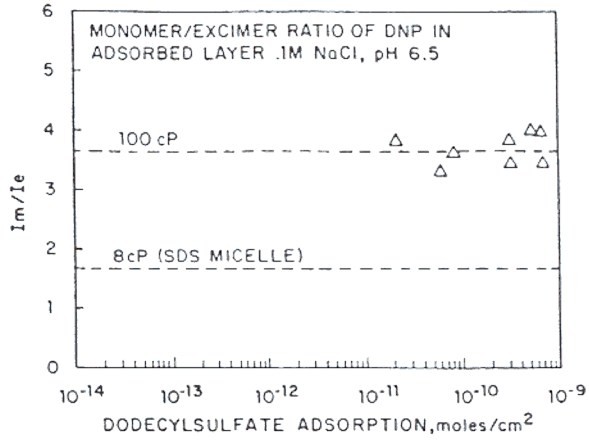

Fig. 5. Monomer to excimer ratio (I_m/I_e) of dinaphthyl propane (DNP) in SDS–alumina slurries as a function of SDS adsorption density. The viscosities refer to those of ethanol–glycerol mixtures which give a similar I_m/I_e ratio for DNP.

marked by an abrupt change in local polarity of the probe from an aqueous environment to a relatively non-polar micelle type environment. It is to be noted that this abrupt change occurs in a region that is well below the critical micelle concentration (CMC) and coincides approximately with the transition in the adsorption isotherm from Region I to Region II. In the plateau region the I_3/I_1 value coincides with the maximum value for SDS micellar solutions, indicating completion of aggregation on the surface. It can also be seen that the polarity parameter is fairly constant throughout most of Region III and above and hence seems to be independent of surface coverage.

Information on microviscosity is obtained by studying the excimer (excited dimer) forming capabilities of suitable fluorescent molecules like 1,3-dinaphthyl propane (DNP). The excimer, which is a complex of a ground state and an excited state monomer, has a characteristic emission frequency. The intramolecular excimer formation is a sensitive function of the microviscosity of its neighborhood. This property, expressed as the ratio of the monomer and excimer yield (I_e/I_m) for 1,3-dinaphthyl propane, is determined for the solution and for the adsorbed layer for the various regions of the adsorption isotherm (Fig. 5) [11]. These are then compared to the I_e/I_m values of DNP in mixtures of ethanol and glycerol of known viscosities. Based on the I_e/I_m values of DNP for ethanol–glycerol mixtures, a microviscosity value of 90–120 cP is obtained for the adsorbed layer compared to a value of 8 cP for micelles. The constancy of microviscosity as reported by DNP is indicative of the existence of a condensed surfactant assembly that holds the probe.

The dynamics of fluorescence emission of pyrene has been previously studied in homogeneous and micellar solutions using time-resolved fluorescence spectrometry [12]. While the decay kinetics of monomer and excimer emission may be derived directly for a homogeneous solution (continuous medium), statistical methods are to be applied to arrive at similar kinetics in aggregated micellar ensembles. This stems from a need to recognize the possibility of random multiple occupancy of the probe in the aggregates which affects the excimer forming probability within the aggregate. If the micellar system is viewed as groups of individual micelles with n probes, then P_n, the average number of probes per micelle, may be related to n by Poisson statistics through the relation

$$P_n = n^n \exp(-n)/n!$$

This model yields the following relation for the time dependence of monomer emission:

$$I_{m[t]} = I_{m[0]} \exp[-k_0 t + n(\exp(-k_e t) - 1)]$$

where k_0 is the reciprocal lifetime of excited pyrene in the absence of excimer formation, k_e is the

intramicellar encounter frequency of pyrene in excited and ground states, and $I_{m[0]}$ and $I_{m[t]}$ represent the intensity of monomer emissions at time zero and time t respectively. Knowing n, one can calculate the aggregation number N using the expression

$$n = [P]/[Agg] = [P]N/([S] - [S_{eq}])$$

where [P] is the total pyrene concentration, [Agg] is the concentration of the aggregates and $[S] - [S_{eq}]$ is the concentration of the adsorbed surfactant.

A kinetic analysis based on this relation of the decay profiles of pyrene in the adsorbed layer for different regions of the alumina/dodecyl sulfate adsorption isotherm [13] yielded the aggregation numbers marked in Fig. 6 for dodecyl sulfate solloids. These results yield a picture of the evolution of the adsorbed layer. The aggregates in Region II appear to be of relatively uniform size while in Region III there is a marked growth in the aggregate size. In Region II, the surface is not fully covered and enough positive sites remain as adsorption sites. Since the aggregation number is fairly constant in Region II, further adsorption in this region can be considered to occur by the formation of more aggregates but of the same size. The transition from Region II to III corresponds to the isoelectric point of the mineral, and adsorption in Region III is proposed to occur through the growth of existing aggregates rather than the formation of new ones due to lack of positive adsorption sites. This is possible by the hydrophobic interaction between the hydrocarbon tails of the already adsorbed surfactant molecule and the adsorbing ones. The new molecules adsorbing at the solid–liquid interface can be expected to orient with the ionic head toward the water since the solid particles possess a net negative charge under these conditions. The whole process of adsorption has been portrayed schematically in Fig. 3.

2.2. *Effect of position of functional group on adsorbed layer microstructure [14]*

Studies of changes in the position of the sulfonate and the methyl groups on the aromatic ring of

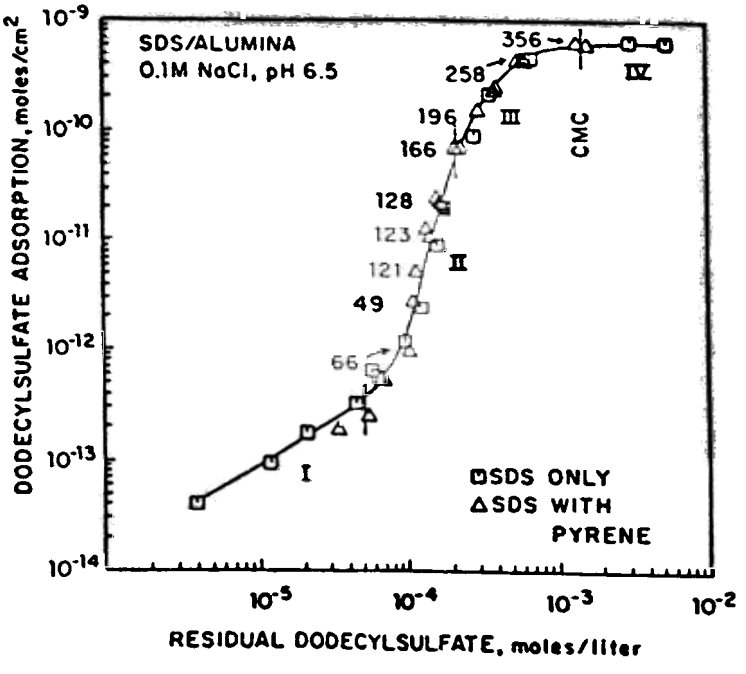

Fig. 6. Surfactant aggregation numbers determined for various adsorption densities (average number is indicated).

alkylxylenesulfonate showed a marked effect of such changes on the micellization and adsorption at the solid–liquid interface. Fluorescence spectroscopy was used to probe the microstructure of the adsorbed layers in these systems. Adsorption isotherms for 4C11 3,5-*para*-xylenesulfonate (Para-1), 4C11 2,5-*para*-xylenesulfonate (Para-2) and 4C11 2,4-*meta*-xylenesulfonate (Meta) on alumina from water and the I_3/I_1 values along various points in the isotherm are shown in Figs. 7 and 8 respectively. At low adsorption densities, I_3/I_1 is about 0.6. Once the solloids form, the value goes up to

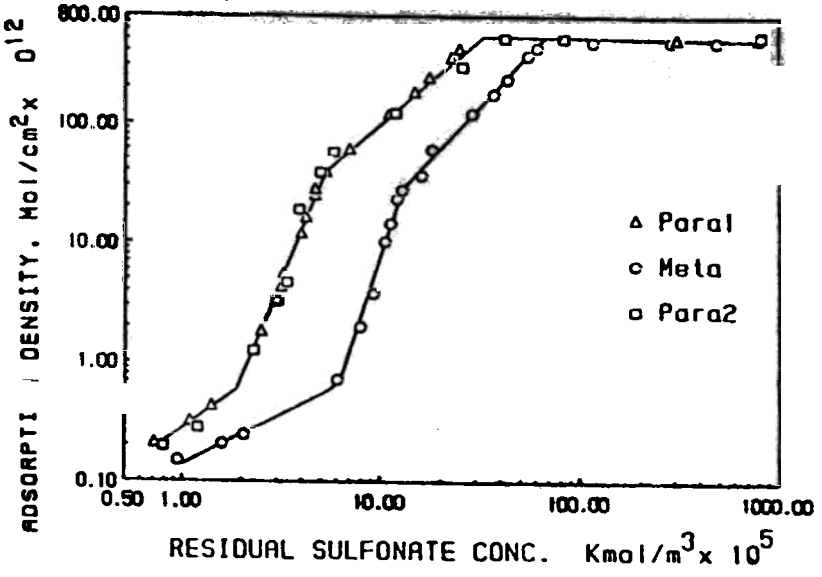

Fig. 7. Adsorption of alkylxylenesulfonates on alumina.

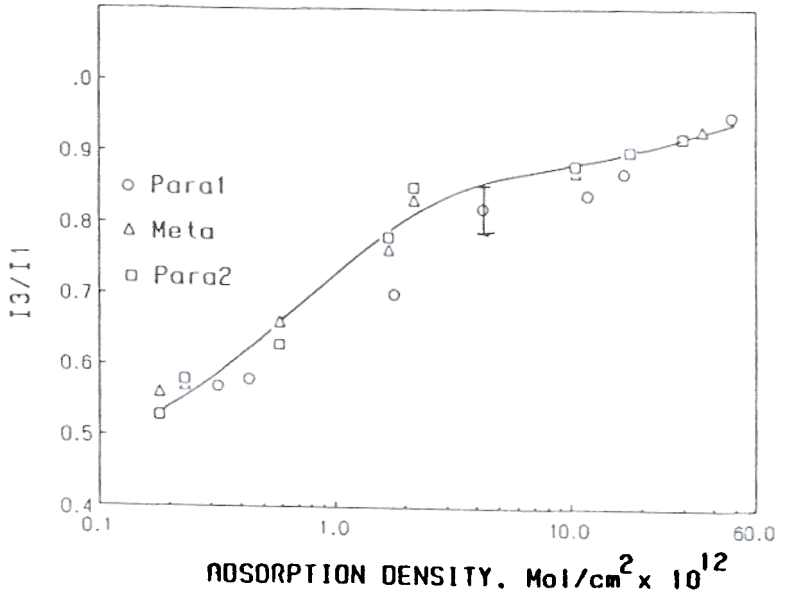

Fig. 8. Polarity of adsorbed layers of alkylxylenesulfonates in terms of I_3/I_1 as a function of surfactant adsorption densit

about 1. It can also be seen that there is no difference among the polarities of the adsorbed layers of the three surfactants indicating that these layers in all three cases are really compact and hence water penetration is the same in all the cases. Average aggregation numbers of the solloids increase from 17 to 76 with increase in adsorption in all the three cases (Fig. 9). The aggregation numbers of the two *para*-xylenesulfonates are similar throughout the range studied. However, at higher adsorption densities, the aggregation number of the *meta*-xylenesulfonate is lower than that of the *para*-xylenesulfonates. This suggests higher steric hindrance to the packing of the surfactant molecules in the solloids of the *meta*-xylenesulfonate. Based on this evidence, the effect of change of position of functional groups on the aromatic ring of the alkylxylenesulfonates on adsorption can be attributed to the steric constraints to the packing of surfactant molecules in their aggregates.

2.3. Polymer conformation in the adsorbed state

Polymers can exist in different conformations both in solution and in the adsorbed state. The adsorption of polymeric materials onto solid surfaces can be quite different from the adsorption of small molecules in that the polymer adsorption is greatly influenced by the multifunctional groups that it possesses [15]. This stems from the widely varying sizes and configurations available for the polymer. In addition, macromolecules usually possess many functional groups each having a potential to adsorb on one or more given surfaces.

Among the polymeric materials, polyelectrolytes are the most important because of their participation in many biological processes and their utility in processes like dispersion, flocculation, adhesion and rheology. Poly(acrylic acid) (PAA) and poly(methacrylic acid) (PMAA) are usually chosen as simple examples of polyelectrolytes to gain insight into the adsorption behavior of polyelectrolytes. Such an understanding is important in acquiring effective control over the processes of colloidal stabilization and flocculation.

Poly(acrylic acid) can exist in different conformations depending on the solvent, pH and ionic strength conditions (Fig. 10) [16]. Such a flexibility also influences its adsorption characteristics on solids and in turn affects the subsequent suspension behavior. Using a fluorescent labelled polymer and by monitoring the extent of excimer formation it was shown that the polymer at the interface could have a stretched or coiled conformation at the

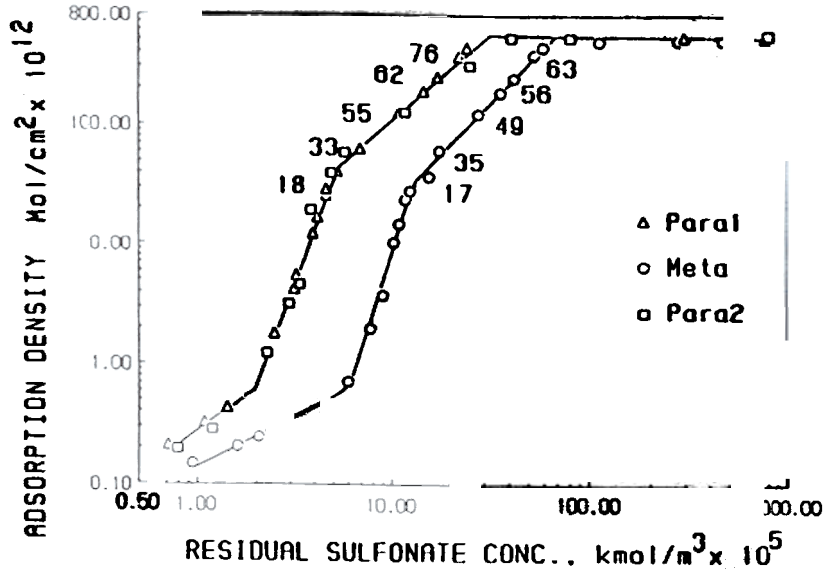

Fig. 9. Aggregation numbers determined at different adsorption densities shown along the isotherm.

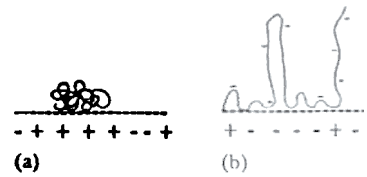

Fig. 10. Schematic representation of the conformation of poly (acrylic acid) at different pH values: (a) pH 4.4; (b) pH 10.5.

interface depending on the pH. The rationale behind the use of this technique is the observation that the extent of excimer formation which depends on the interaction of an excited state pyrene of the polymer pendant group with another pyrene group in the ground state has a direct bearing upon the polymer conformation. This may be understood with reference to Fig. 11 which shows that at low pH there is a better probability for intramolecular excimer formation between pyrene groups resulting from a favorable coiled conformation. Similarly a low probability for excimer formation at high pH may be understood as a consequence of the repulsion between the highly ionized carboxylate groups in the polymer and the subsequent stretching of the polymer chain. This difference is reflected in the nature of their fluorescence spectra as seen in Fig. 12. Also these studies have demonstrated that the poly(acrylic acid) adsorbed in the stretched form on alumina at high pH was essentially irreversible as the conformation could not be altered by lowering the pH subsequently (Fig. 13) [17]. In contrast, the polymer adsorbed in the coiled form at low pH did stretch out when the pH was increased.

We have also performed a detailed investigation on the flocculation behavior of alumina particles

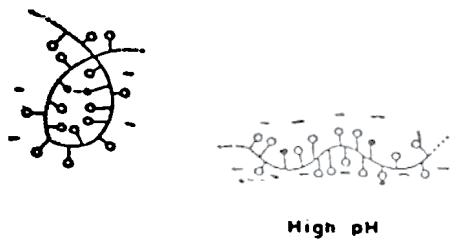

Fig. 11. Schematic representation of the correlation of the extent of excimer formation and intrastrand coiling of pyrene-labeled poly(acrylic acid).

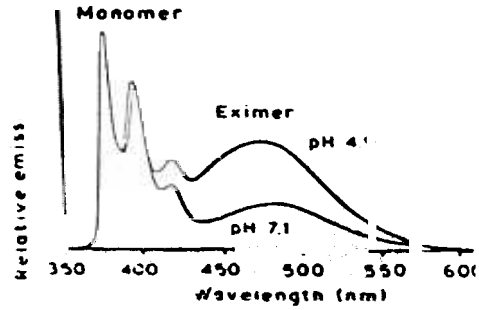

Fig. 12. Fluorescence emission spectra of adsorbed polymer at two pH values.

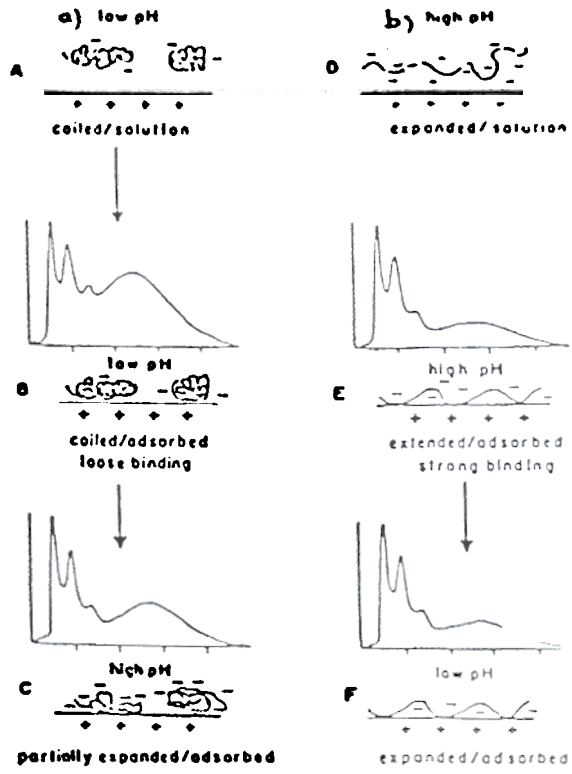

Fig. 13. Schematic representation of the adsorption process of pyrene-labeled poly(acrylic acid) on alumina. A, At low pH polymer is coiled in solution which leads to B, adsorption in coiled form. C, Subsequent raising of the pH causes some expansion of the polymer. D, Polymer at high pH in solution is extended and E, binds strongly to the surface in this conformation. (F). Subsequent lowering of pH does not allow for sufficient intrastrand interactions for coiling to occur.

with and without added polymer under fixed and shifted pH conditions. The polymer conformation was shown to be a controlling factor of the flocculation process in this case. The results of fluorescence emission studies using pyrene-labeled PAA in the adsorbed state under shifted pH conditions, i.e. adsorbing the polymer at a fixed pH and then changing the pH to a desired value, are shown in Fig. 14. It may be noted that the excimer fluorescence emission intensity of the solid/liquid equilibria after adsorption at high pH values remains the same even after changing the pH to lower values. From this observation, coupled with the above results, the variation of poly(acrylic acid) conformation at the solid–liquid interface under shifted pH conditions may be represented as shown in Fig. 15. It may be inferred that the polymer conformation at a given pH may be manipulated by controlling the adsorption conditions.

2.4. Polymer orientation in non-aqueous media

Fluorescence spectroscopy was also used to detect polymer orientation on particles in non-aqueous media. 7-Dimethylamino-4-methylcoumarin which is a relatively hydrophilic molecule was used to probe the adsorbed layer of DAPRAL GE 202 (maleic anhydride–α-olefin copolymer with both hydrophobic and hydrophilic side-chains) at the alumina–toluene interface. The spectrum for the probe in the absence of DAPRAL is similar to that obtained in water solution (maximum emission at 470 nm, Fig. 16). This is attributed to the hydrophilicity of the bare alumina surface. With an increase in polymer adsorption, the maximum wavelength shifts toward the shorter wavelength range reaching the value for hydrocarbon solvents (390 nm) at 500 mg l^{-1} of DAPRAL (Fig. 17). This observation supports the mechanism of polymer adsorption through the interaction between the ethylene oxide chains and the hydroxyl groups on the alumina surface with the hydrocarbon side-chains dangling toward the solution and the alumina particles eventually fully covered to become totally hydrophobic. This is also evidenced by the fact that the alumina suspensions are stabilized significantly by the adsorption of DAPRAL.

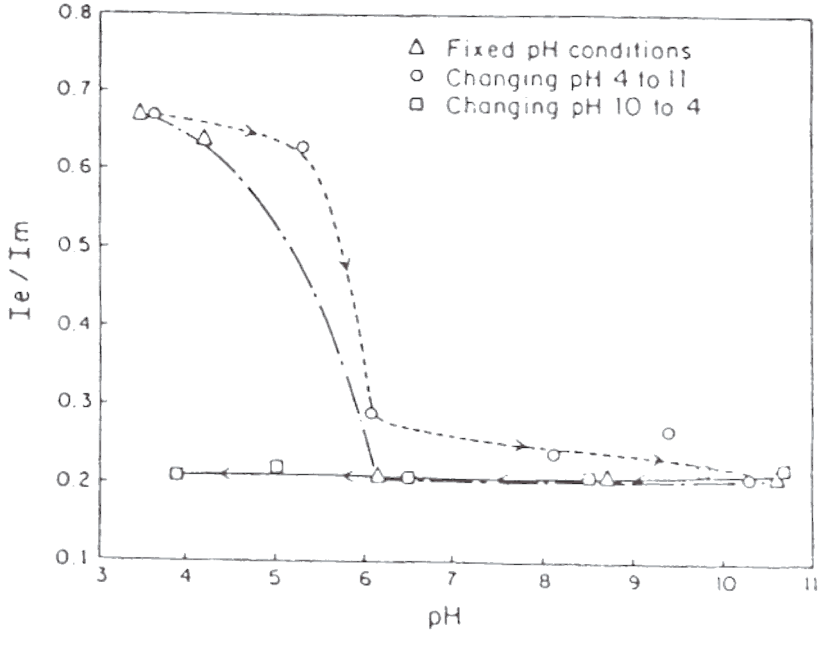

Fig. 14. Excimer to monomer ratio I_{e} $_{m}$ for alumina with 20 ppm poly(acr acid) as a function of final pH under changing pH conditions.

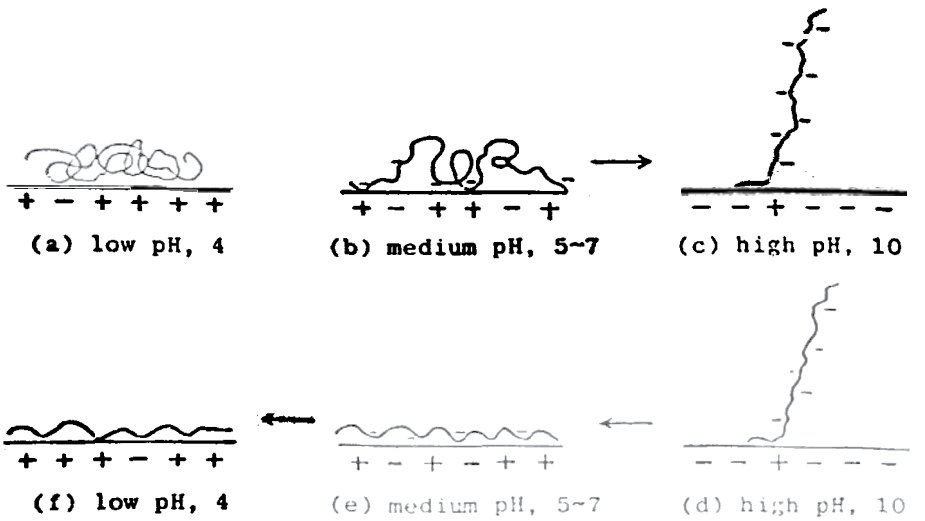

Fig. 15. Schematic representation of the variation of polymer conformation at the solid liquid interface under changing pH conditions.

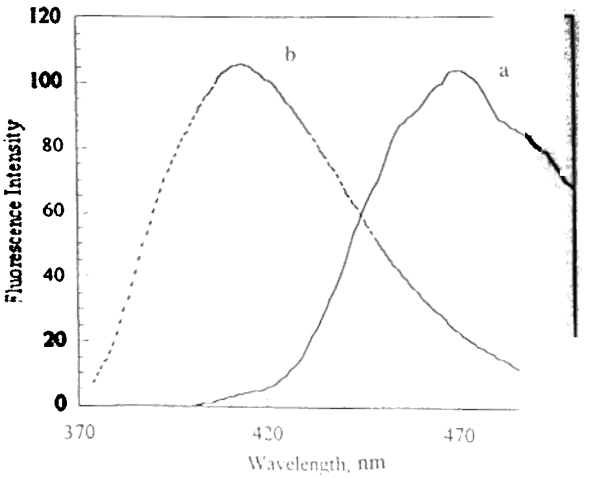

Fig. 16. Fluorescence spectrum of 7-amino-4-methylcoumarin at the alumina–toluene interface in the presence of 0 ppm DAPRAL (curve a) and 100 ppm DAPRAL (curve b).

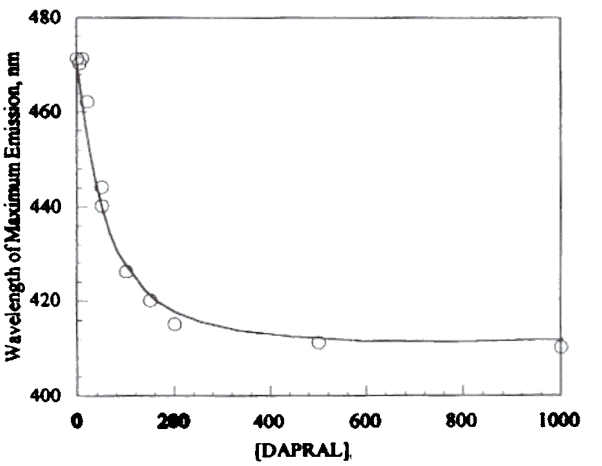

Fig. 17. Diagram illustrating the shift in maximum emission wavelength of coumarin at the alumina–toluene interface with adsorption of DAPRAL.

3. Electron spin resonance spectroscopy (ESR)

ESR studies as applied to micellar systems rely on the sensitivity of a free radical probe to respond to its microenvironment. Molecular species with a free electron possess intrinsic angular momentum (spins), which in an external magnetic field undergoes Zeeman splitting. For a system with $S = 1/2$, two Zeeman energy levels are possible whose energy gap (ΔE) is given by

$$E = h\nu = gBH_0$$

The magnetic moment of the free electron is susceptible also to the secondary magnetic moments of the nuclei and thus the Zeeman splitting will be superimposed by the hyperfine splitting which brings about further splitting of the absorption signal. The hyperfine splitting pattern depends on

the spins and the actual number of the neighboring nuclei with spins. If the electron is in the field of a proton then the ESR spectrum would yield two lines of equal intensity, and similar interaction by a nucleus with $S = 1$, as in nitrogen, would produce a triplet of equal intensity. The line shapes of ESR signals are subject to various relaxation processes (spin–lattice and spin–spin relaxations) occurring within the spin system as well as anisotropic effects due to the differentially oriented paramagnetic centers being acted upon by an external magnetic field [18]. These effects result in a broadening of the absorption lines. Three types of ESR study can be applied to probe surfactant microstructures–spin probing, spin labeling and spin trapping [19]. In the spin probing technique, a molecule with spin is externally added to the system, whereas in spin labeling a spin-bearing moiety, through covalent bonding, part a part of the molecule. The spin trapping technique is mainly used for the identification of radicals produced thermally, photochemically or radiolytically by trapping the radical through chemical reactions with a spin trap (like butyl nitroxide) and converting the radical to a free radical which can be examined by ESR. In this study, three isomeric stable free radicals 5-, 12- and 16-DOXYL-stearic acids were used as the spin labels. These spin labels were co-adsorbed individually on the alumina along with the main adsorbate, sodium dodecyl sulfate, and the main regions of the isotherm were investigated.

Information on micropolarity and microviscosity can be obtained by measuring the hyperfine splitting constant A_N and the rotational correlation time τ_c. The latter is a measure of the time required for a complete rotation of the nitroxide radical about its axis. Its value can be defined as the time required for the nitroxide to rotate through an angle of one radian. The hyperfine splitting constants of 16-DOXYL-stearic acid measured in dodecylsulfonate solloids (hemi-micelles) (15.0 G) is indicative of a less polar environment in comparison to its value for water (16.0 G) and SDS micelles (15.6 G) (Fig. 18). Similarly microviscosities esti-

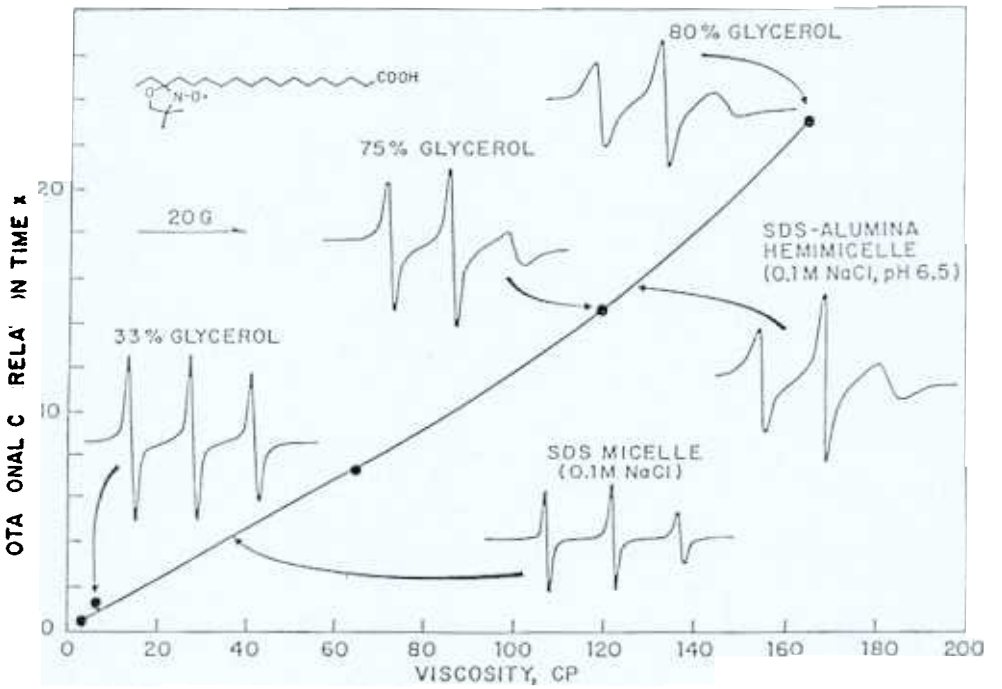

Fig. 18. Comparison of ESR spectra of 16-DOXYL-stearic acid in solloids, micelles and ethanol–glycerol mixtures and corresponding rotational correlation times and viscosities.

mated from τ_c measurements and calibrated against τ_c measured in ethanol–glycerol mixtures give reasonably high values for the solloids relative to the values for water. Three different microviscosities were obtained using different probes in the solloids, indicating that the nitroxide group in each case experienced a different viscosity within the solloid. These observations may be explained by assuming a model for the adsorption of the probe in which the carboxylate group is bound to the alumina surface. Such a model would require us to attribute greater mobility for the nitroxide moiety near the SDS–H_2O interface (as in the 16-DOXYL-stearic acid case) and less mobility for the 12-DOXYL and 5-DOXYL cases [20,21]. This work is the first reported indication of variations in microviscosity within a surfactant solloid as estimated by any known technique.

3.1. *Conformation of adsorbed Aerosol-OT at the alumina–cyclohexane interface [22,23]*

Colloidal dispersions in non-aqueous media have a number of technological applications and water is present in most of these cases and plays a major role in determining the dispersion behavior. The effect of water on the stability of a colloidal suspension of alumina in cyclohexane in the presence of surfactant, Aerosol-OT is shown in Fig. 19. A succession of flocculated, dispersed and flocculated states is observed as the amount of water added to the suspensions is increased. ESR studies were conducted using 7-DOXYL-stearic acid as a probe to get structural information on the adsorbed layer. Fig. 20 shows ESR spectra of 7-DOXYL-stearic acid adsorbed on alumina in the presence and absence of adsorbed surfactant. The values of $A_{\parallel}$ obtained in the two cases, 69 G and 65 G, respectively, are significantly different from each other, suggesting that despite the slow motion of the probe it is possible to distinguish between the probe interacting directly with the mineral surface and that hindered in its motion by the surfactant molecules surrounding it.

Fig. 21 shows some of the spectra obtained at different water concentrations with 7-DOXYL-stearic acid co-adsorbed with a full monolayer of Aerosol-OT on the alumina surface. The changes observed in the ESR line shape correspond to an increase in probe mobility consistent with a decrease in the ordering of the probe environment. These observed changes are quantified by using the concept of order parameter S which can be calculated from the spectrum using the following equation:

$$S = 1.66\,\frac{\{A_{\parallel} - [A_i(\text{meas}) + C]\}}{\{A_{\parallel} + 2[A_i(\text{meas}) + C]\}}$$

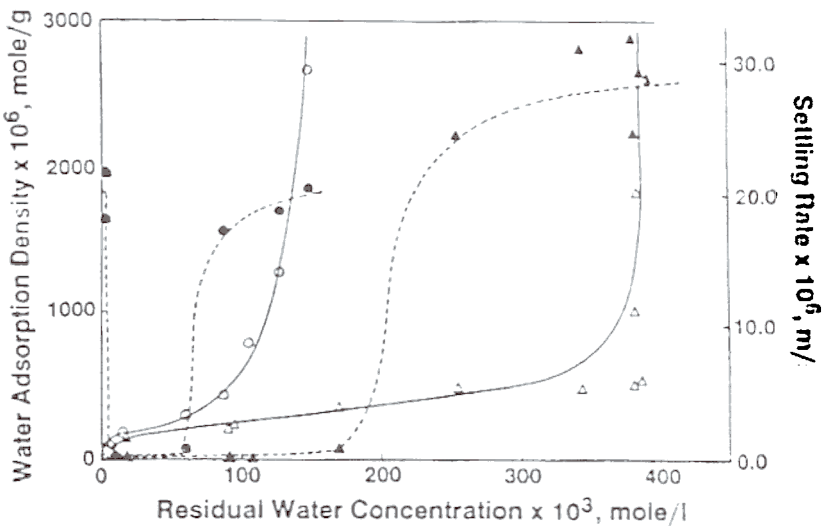

Fig. 19. Effect of water on the alumina suspension stability at two different surfactant concentrations: solid symbols, [AOT] = 8.5×10^{-3} M; empty symbols, [AOT] = 26.5×10^{-3} M.

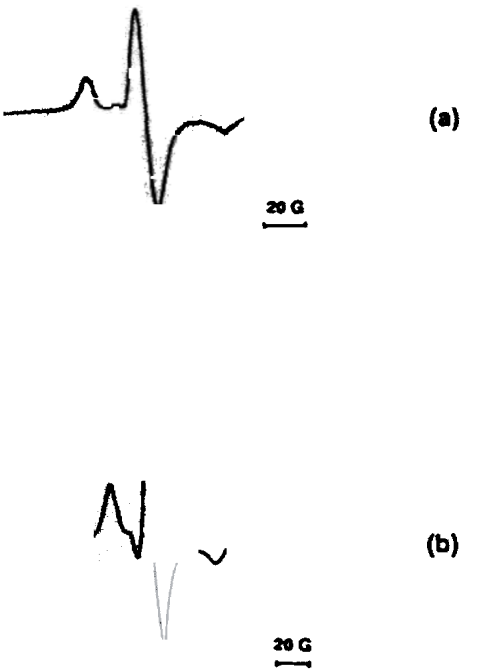

Fig. 20. ESR spectra of 7-DOXYL-stearic acid probe adsorbed on alumina in the absence (a) and presence (b) of Aerosol-OT.

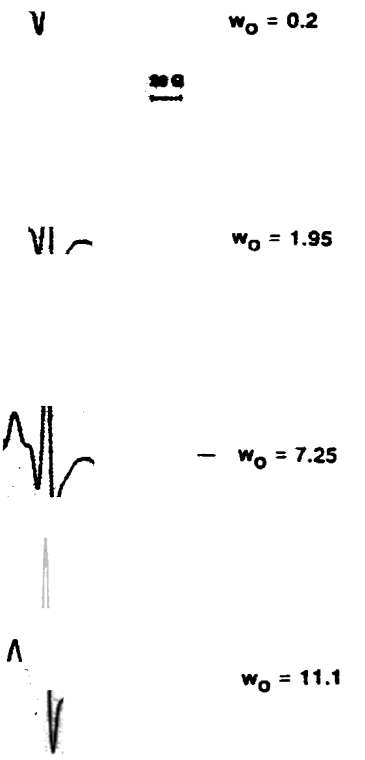

Fig. 21. Effect of water on the ESR spectra of 7-DOXYL-stearic acid co-adsorbed with a monolayer of Aerosol-OT at the alumina–cyclohexane interface.

where $C = 1.45 - 0.019[A_{\parallel} - A_{\parallel}(\text{meas})]$ G. The order parameter is usually a parameter of molecular motion. S varies between 0 (low order) and 1 (high order). The calculated parameter plotted as a function of water concentration is shown in Fig. 22. It can be seen that as more water is added to the suspension the order parameter decreased until it reached a constant value of 0.75. These results are interpreted in terms of an increase in the probe lateral diffusion within the adsorbed surfactant layer. Such an increase in the probe lateral diffusion is realistic, considering the structural reorganization of the complex adsorbed layer when water is present at the interface. At low water concentrations, water molecules bind the carboxylic groups of the stearic acid molecules and the polar groups of Aerosol OT, directly to the hydroxyl groups of the alumina surface. This binding limits the ability of the probe to move within the adsorbed layer and is consistent with a model of localized adsorption where the adsorbed molecules have limited degrees of freedom. As the water adsorption density increases, the carboxylic groups of the probe molecules interact with water molecules not bound directly to the hydroxyl groups of the mineral surface. Similar interactions between the polar groups of Aerosol-OT and water molecules are most likely, as a result of which the adsorbed layer can become loosely bound to the mineral surface. The molecular diffusion limited by the binding of the surfactant molecules at low water concentrations thus increases markedly as water adsorbs on particles.

4. Raman spectroscopy

Raman spectroscopy is acclaimed as a vibrational technique well suited for studies of aqueous

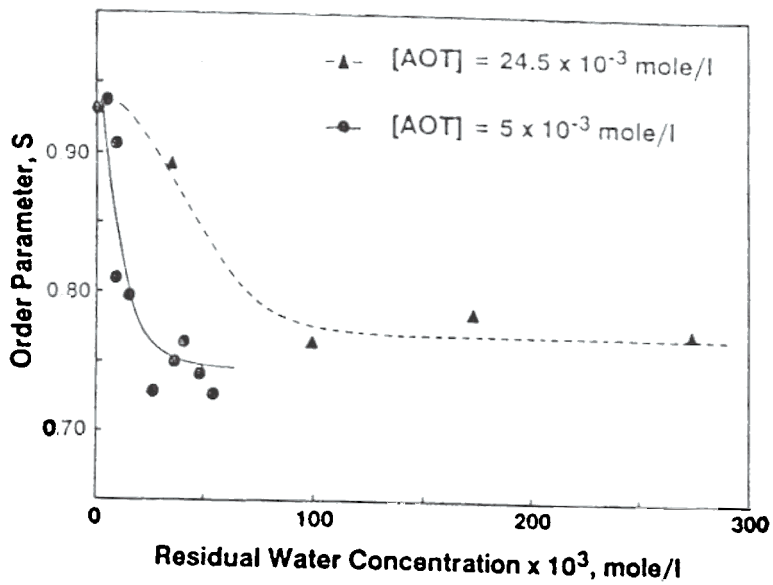

Fig. 22. Effect of water on the order parameter S, calculated from the ESR spectra of 7-DOXYL-stearic acid co-adsorbed with Aerosol-OT at the alumina–cyclohexane interface.

environments compared to IR owing to the near transparency of the former and the ease with which the whole vibrational region of interest can be covered. Vibrational frequencies of molecules in the bound state should be different from those in the free state. Also, it is susceptible to changes in the symmetry properties of the environment. Very few definitive studies exist in the literature concerning the Raman spectroscopy of surfactants in solution. Raman investigations of surfactant adsorbates are reported as surface-enhanced Raman studies at the metal colloid–or metal electrode–liquid interface.

The alumina–dodecylsulfate system has also been probed by excited state resonance Raman spectroscopy using tris(2,2′-bipyridyl) ruthenium(II) chloride, $Ru(bpy)_3^{2+}$, as a reporter molecule [24]. It has been shown that ruthenium polypyridyl complexes serve as excellent photophysical probes for biopolymers like nucleic acids. The excited state of $Ru(bpy)_3^{2+}$ shows strong resonance-enhanced Raman transitions when probed at 355 nm. Furthermore, it has been shown that binding of this ion to clay particles results in substantial changes in the ground state transitions of the excited state resonance Raman spectrum. For these reasons this probe was chosen to study the solloids formed at the alumina–water interface with excited state resonance Raman spectroscopy.

Raman spectra of $Ru(bpy)_3^{2+}$ above the CMC show frequency shifts as well as intensity changes as compared to its spectrum in water. Table 1 lists the relative intensities of various lines with respect to the line at 1286 cm^{-1} in water. These transitions can be attributed to the perturbation of the excited

Table 1
Normalized intensities for various Raman transitions in aqueous solution and SDS micelles

Peak position (cm^{-1})	Normalized intensity	
	Aqueous solution (±3%)	SDS micelles (±3%)
1213	0.66	0.84
1286	1.00	1.00
1324	0.11	0.20
1426	0.42	0.42
1499	0.47	0.73
1547	0.85	0.92
1605	0.26	0.39

state by the SDS micelles. The excited state resonance Raman spectrum of this probe in various regions of the adsorption isotherm for the alumina–SDS system is shown in Fig. 23. The

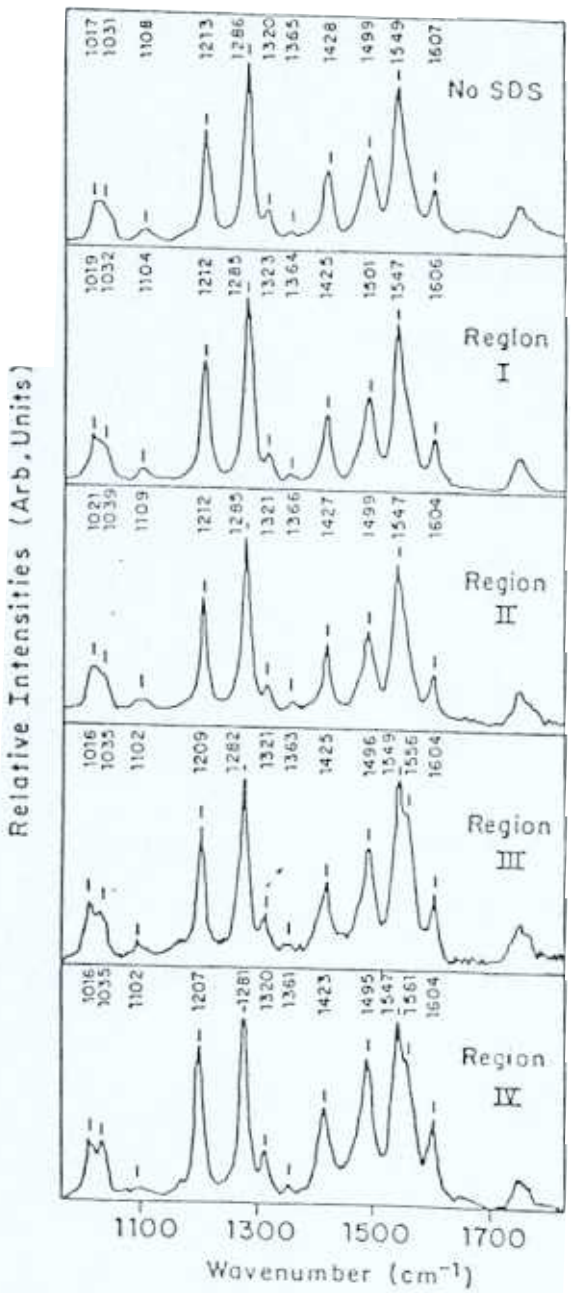

Fig. 23. Resonance Raman spectrum of $Ru(bpy)_3^{2+}$ for various regions of the alumina–SDS adsorption system.

spectrum of $Ru(bpy)_3^{2+}$ on alumina in the absence of SDS is very similar to its spectrum in water both in terms of frequencies and relative intensities. This trend is continued into Region II, where the solloid aggregation process starts. In Regions III and IV, the Raman spectrum shows significant changes. The frequency shifts are more pronounced than in the case of micelles. A plot of change in wavenumbers for some of the lines in the four different regions of the adsorption isotherm is shown in Fig. 24. The changes in Raman frequency and intensity assume substantial significance in the transition Regions II and III onward only. This could be due to the change of net charge on the alumina surface from positive to negative. The favorable net negative charge enhances the adsorption of the probe at the solid–liquid interface. Accordingly, no adsorption of $Ru(bpy)_3^{2+}$ was observed when the supernatants were analyzed in Region I and Region II or in the absence of SDS. These results indicate that adsorption of $Ru(bpy)_3^{2+}$ on to alumina becomes significant only close to the point of zero charge. The transitions at 1213, 1286 and 1428 cm^{-1} show significant increments and these trends clearly suggest the probe adsorption on to the solloids. Also it was

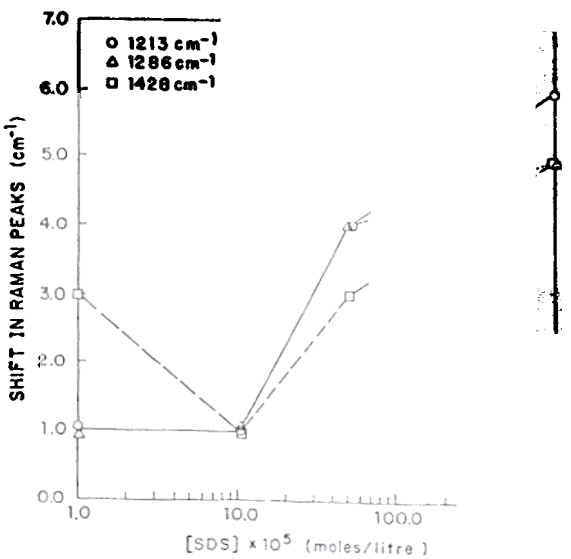

Fig. 24. Frequency shifts of resonance Raman lines of $Ru(bpy)_3^{2+}$ as a function of SDS concentration for an alumina–SDS system.

seen that the 1286 peak shifted to 1281 in the presence of solloids while it was practically unchanged in the SDS micelles. It may be speculated that $Ru(bpy)_3^{2+}$ may be sensing different environments within the SDS micelles and the alumina–SDS solloids. Implicit in these results is also the potential of time-resolved Raman spectroscopy as a powerful diagnostic tool to explore the solid–liquid interface.

5. Conclusions

The use of various spectroscopic techniques for studying the adsorbed layers of surfactants and polymers in aqueous and non-aqueous systems is elucidated here. A number of new findings are reported with regard to the structure and evolution of surfactant and polymer solloids by an integrated approach using the classical bulk property measurements and the modern spectroscopic techniques. The aggregation number of SDS on alumina was determined at various points during solloid evolution and the variation of the microviscosity within the solloid layer determined along the isotherm. Fluorescence spectroscopic studies also indicate that steric hindrance to packing in the adsorbed layers controls solloid formation of the alkylxylenesulfonates. The effect of pH-dependent conformational equilibria of poly(acrylic acid) on the adsorption process and its implications to flocculation have been explored to suggest reasonable conformational structures for the polymer solloid. Finally, the role of water in controlling the dispersion properties of alumina dispersed in cyclohexane by increasing the lateral diffusion of the adsorbed surfactant molecules was depicted using the ESR technique. It is clear that there is a variety of techniques now becoming available to examine structures in situ at levels smaller than ever before. With technologies now being developed to examine interfaces at atomic scales and dynamics of these atoms and molecules at pico and femto scales, opportunities will arise to visualize processes such as aggregation and reaction between various species at interfaces as they take place.

Acknowledgments

The authors wish to acknowledge the National Science Foundation, the Department of Energy, Unilever Research, Engelhard Co., NALCO and ARCO for their financial support.

References

[1] P. Somasundaran, AIChE Symp. Ser., (1975) 71.
[2] P. Somasundaran, T.W. Healy and D.W. Fuerstenau, J. Phys. Chem., 68 (1964) 3562.
[3] J.R. Lakowicz, Principles of Fluorescence Spectroscopy, Plenum, New York, 1983.
[4] J.K. Thomas, The Chemistry of Excitation at Interfaces, American Chemical Society Monograph, 1984.
[5] N.J. Turro, G.S. Cox and M.A. Paczkowski, Top. Curr. Chem., 129 (1985) 57.
[6] P. Somasundaran and D.W. Fuerstenau, J. Phys. Chem., 70 (1966) 90.
[7] A.M. Gaudin and D.W. Fuerstenau, Min. Eng., 7 (1955) 66.
[8] P. Somasundaran and D.W. Fuerstenau, J. Phys. Chem., 70 (1966) 90.
[9] P. Somasundaran and J.T. Kunjappu, Colloids Surfaces, 37 (1989) 245.
[10] J.H. Harwell and D. Bitting, Langmuir, 3 (1987) 500.
[11] P. Somasundaran, P. Chandar and N.J. Turro, Colloids Surfaces, 20 (1986) 145.
[12] J.N. Demas, Excited state lifetime measurements, Academic Press, New York, 1983.
[13] P. Chandar, P. Somasundaran and N.J. Turro, J. Colloid Interface Sci., 117 (1987) 31.
[14] A. Sivakumar and P. Somasundaran, Langmuir, 10 (1994) 131.
[15] H. Morawetx, Macromolecules in Solution, Wiley, New York, 1975.
[16] K.S. Arora and N.J. Turro, J. Polym. Sci., 25 (1987) 243.
[17] P. Chandar, P. Somasundaran, K.C. Waterman and N.J. Turro, Langmuir, 3 (1987) 298.
[18] J.H. Wertz and J.R. Bolton, Electron Spin Resonance–Elementary Theory and Practical Applications, Chapman and Hall, New York, 1986.
[19] B. Ranby, in J.K. Rabek (Ed.), ESR Spectroscopy in Polymer Research, Springer-Verlag, Berlin, 1977.
[20] K.C. Waterman, N.J. Turro, P. Chandar and P. Somasundaran, J. Phys. Chem., 90 (1986) 6829.
[21] P. Chandar, P. Somasundaran, K.C. Waterman and N.J. Turro, J. Phys. Chem., 91 (1986) 150.
[22] C.A. Malbrel, D. Eng. Sci. Thesis, Columbia University, New York, 1991.
[23] C.A. Malbrel and P. Somasundaran, Langmuir, 8 (1992) 1285.
[24] P. Somasundaran, J.T. Kunjappu, C.V. Kumar, N.J. Turro and J.K. Barton, Langmuir, 5 (1989) 215.